Simulation of Crystallization Analysis Fractionation (Crystaf) of Linear Olefin Block Copolymers

Siripon Anantawaraskul,[1] *Punnawit Somnukguande,*[1] *João B. P. Soares**[2]

Summary: Linear olefin block copolymers (OBCs) have microstructures that are unique among polyolefins and exhibit properties that are different from those of other polyolefin elastomers. Characterizing their chain microstructures is a challenging task, as conventional characterization techniques cannot probe directly block length distribution or composition. In this work, we used a Monte Carlo model to predict the microstructure details of OBCs and a modified version of the Crystaf model previously developed in our groups to describe theoretical Crystaf profiles for model OBCs. This model can be used as a tool to interpret Crystaf results of these interesting new polyolefins and to relate them to OBC microstructures. Effects of polymerization parameters on OBC microstructure and Crystaf profiles were also discussed.

Keywords: chain shuttling; Crystaf; crystallization analysis fractionation; olefin block copolymers; polyethylene elastomers

Introduction

Linear olefin block copolymers (OBC) constitute a new class of polyolefins produced using chain shuttling catalyst technology.[1,2] Chain shuttling polymerization uses two catalysts with different comonomer reactivity ratios in combination with a chain shuttling agent (CSA). The CSA acts as a reversible chain transfer agent, ''shuttling'' polymer chains between the two catalysts and producing linear block copolymer chains with a statistical distribution of block sizes and number of blocks per chain. For an ethylene/α-olefin copolymer, the catalyst with the high comonomer reactivity ratio may be used to produce soft or low-crystallinity blocks, while the catalyst with the low comonomer reactivity ratio makes hard or high-crystallinity blocks. These linear block olefin copolymers have been claimed to have novel end-use properties (such as higher heat and abrasion resistances) and enhanced processability, providing advantages over conventional polyolefin elastomers.

While the crystallization and rheological behavior of OBCs have been investigated,[3–5] characterizing their chain microstructure is a challenging task. Even though analytical temperature rising elution fractionation (ATREF) and crystallization analysis fractionation (Crystaf) results have been reported for OBCs,[6] linking these results to chain microstructural distributions is difficult because neither ATREF nor Crystaf can probe directly the block length and composition distributions of these polymers.

Recently, a model for describing Crystaf profiles of random homo- and copolymers was developed in our groups.[7–9] This model has an advantage over previously proposed models[10–15] because it takes crystallization kinetics into account and can describe experimental Crystaf results of random polyolefins measured under different cooling rates very well. The model can provide useful, quantitative insights on the Crystaf fractionation mechanism and its relation to polymer microstructure.

[1] Department of Chemical Engineering, Kasetsart University, 50 Phaholyothin Rd, Jatujak, Bangkok, Thailand 10900

[2] Department of Chemical Engineering, University of Waterloo, Waterloo, Ontario, Canada N2L 3G1
Fax: 001 519-746-4979;
E-mail: jsoares@uwaterloo.ca

In the present publication, we developed a Monte Carlo model to simulate the microstructure of OBCs and used this information to predict their Crystaf profiles using a modified version of our kinetic Crystaf model. Effects of polymerization parameters such as chain shuttling probability, propagation probability, and catalyst ratio on Crystaf profiles were examined from a theoretical perspective. We believe this approach could be useful to infer the chain microstructures of OBCs based on Crystaf analysis.

Model Development

Monte Carlo Simulation of OBC Microstructures

OBC microstructures, as defined by their molecular weight distribution, comonomer fraction, and longest ethylene sequences per chain, were simulated using a Monte Carlo model. Polymer chains were generated following the chain shuttling polymerization mechanism published in the literature[1,2] and illustrated schematically in Figure 1. Random numbers between 0 and 1 were used to select among the different polymerization steps shown in Figure 1. A simplified flowchart for the algorithm used in the Monte Carlo simulations is shown in Figure 2.

To start the formation of a polymer chain, the catalyst type was randomly selected using the molar fraction of Catalyst 1 in the reactor (for simplicity, we assumed that both catalysts had the same overall activity; this hypothesis can be easily relaxed without affecting the general results reported herein). If the random number (R) is less than the mole fraction of Catalyst 1 in the reactor (P_{cat1}), the chain starts growing on Catalyst 1; otherwise, it starts growing on Catalyst 2. In this study, Catalyst 1 was assumed to make ethylene-rich chains, while Catalyst 2 produced α-olefin-rich chains. The first monomer molecule added to the catalyst was selected based on the monomer (P_m) and comonomer (P_c) incorporation probabilities assumed for each catalyst type. If $R \leq P_m/(P_m + P_c)$, ethylene is the first unit to react; otherwise, the α-olefin.

Subsequent reactions taking place at the catalyst, chain propagation, chain shuttling, or chain transfer, were determined by

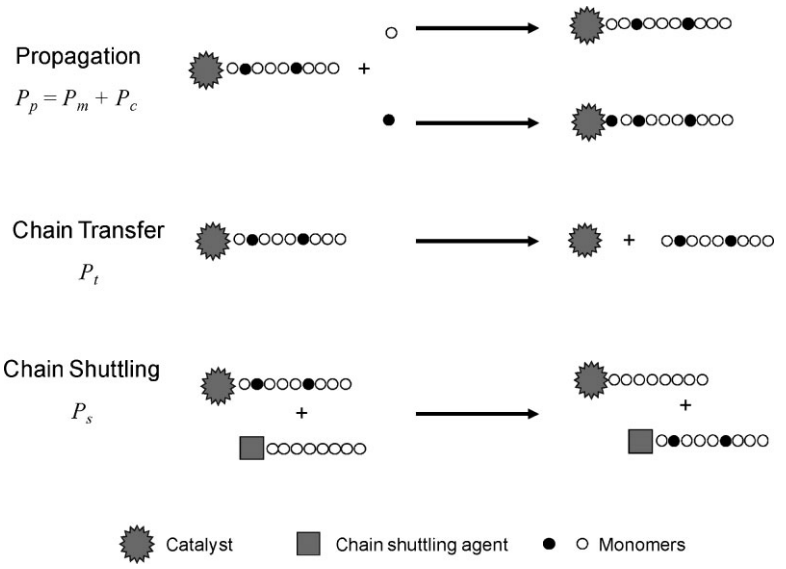

Figure 1.
Chain shuttling polymerization mechanism. Only one catalyst type is illustrated for simplicity.

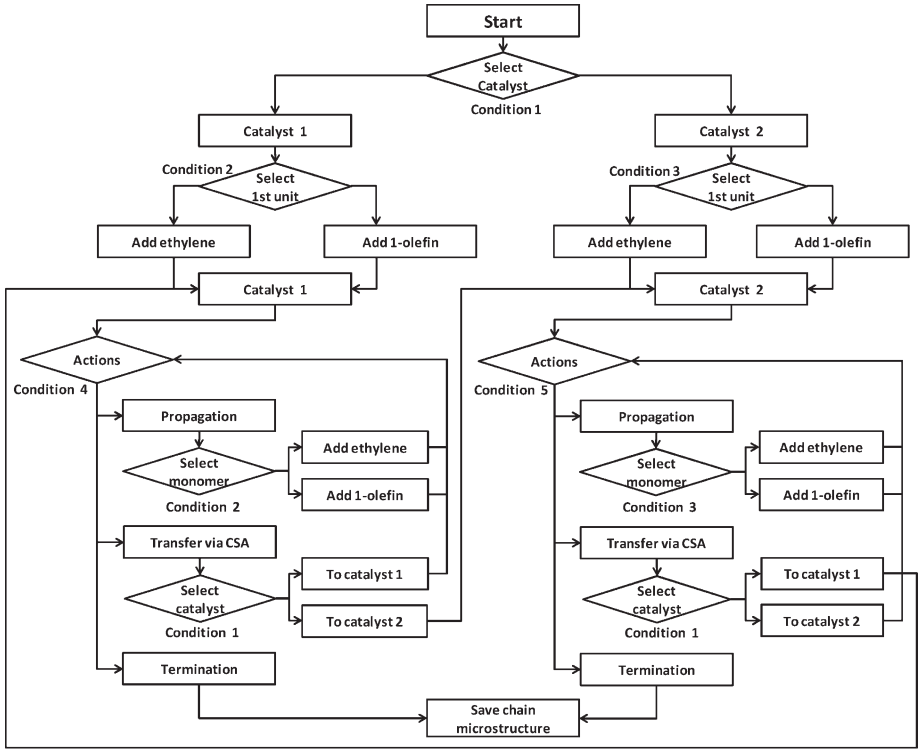

Summary of conditions in the simplified OBC algorithm

Condition 1: If $R \leq P_{cat1}$ then chain starts with Catalyst 1, else chain starts with Catalyst 2

Condition 2: If $R \leq P_{m,1}/(P_{m,1}+P_{c,1})$ then add ethylene unit, else add α-olefin unit

Condition 3: If $R \leq P_{m,2}/(P_{m,2}+P_{c,2})$ then add ethylene unit, else add α-olefin unit

Condition 4: If $R \leq P_{p,1}$ then chain propagates, else if $R \leq P_{p,1} + P_{s,1}$ then chain transfers, else chain terminates

Condition 5: If $R \leq P_{p,2}$ then chain propagates, else if $R \leq P_{p,2} + P_{s,2}$ then chain transfers, else chain terminates

Figure 2.
A simplified Monte Carlo algorithm to simulate the microstructure of OBC copolymers.

comparing another random number with the propagation (P_p), chain shuttling (P_s), and chain transfer probabilities (P_t). A polymer chain propagates if $R \leq P_p$, is shuttled if $P_p < R \leq P_p + P_s$, and terminates otherwise. Note that $P_p + P_s + P_t = 1$ for each catalyst type, since these three probabilities encompass all the possible events taking place during the life time of a polymer chain, as proposed in Figure 1. The parameter P_t is related to the number average chain length, r_n, of polymer produced with a given catalyst type by the relation $P_t = 1/r_n$.

In the case of propagation, another random number is generated to decide which monomer type is incorporated onto the chain. This decision is made by comparing the random number with P_m and P_c. The monomer (ethylene in the present simulations) is considered to be incorporated into the polymer chain when

$R \leq P_m/(P_m + P_c)$; otherwise, the α-olefin is selected for propagation. We assumed that the copolymerization followed Bernoullian statistics, that is, the propagation probability of a given monomer is equal to its average mole fraction in the copolymer. First or higher order Markovian statistics can be easily incorporated into our Monte Carlo algorithm if necessary.

When a polymer chain is selected to react with a chain shuttling agent, another random number is generated to decide to which catalyst type the selected chain will be transferred, according to the molar fractions of Catalyst 1 and Catalyst 2 in the reactor. If the $R \leq P_{cat1}$, the chain is shuttled to another Catalyst 1 molecule and no new block is formed; if $R > P_{cat1}$, the chain is transferred to Catalyst 2, starting the formation of an ethylene/α-olefin block with composition different from the previous one.

This process is repeated until the chain terminates. After chain transfer, information on the chain microstructure is recorded. It is important to note that all probabilities (P_p, P_s, P_t, P_m, and P_c) considered in the model are assumed to be different for each catalyst type. For the simulations discussed in this paper, 200,000 polymer molecules were generated to provide an adequate representation of the OBC microstructure.

Crystaf Model for Random Ethylene/α-Olefin Copolymers

Since the detailed model formulation and validation of Crystaf profiles for random ethylene/α-olefin copolymers have been reported earlier,[7-9] only the key concepts will be reviewed in this section. In the case of random ethylene/α-olefin copolymers, the longest ethylene sequence (*LES*) in each chain, which depends on both molecular weight and comonomer content, is proposed to be the main factor determining chain crystallizability in solution and, consequently, Crystaf profiles.

To simulate Crystaf profiles, polymer chains are separated into several populations with similar *LES*. Assuming that the crystallization kinetics of each population follows the Avrami equation and that the relationship between dissolution temperature and *LES* can be described with the modified Gibbs-Thomson equation, the degree of crystallinity (X) as a function of *LES*, cooling rate (CR), and crystallization temperature (T_C) for each population is given by,

$$X(LES, T_C) = \begin{cases} 0, & T_C \geq T_d(LES) - T_l \\ 1 - \exp\left\{-k\left[\frac{(T_d(LES) - T_l) - T_C}{CR}\right]^n\right\}, & T_C < T_d(LES) - T_l \end{cases} \quad (1)$$

where n is the Avrami exponent, k is the apparent Avrami rate constant, T_l is the temperature lag in the Crystaf oven (which is a function of the cooling rate and given by the expression $T_l = 5.02 \times CR - 0.05$ for our Crystaf unit), and $T_d(LES)$ is the dissolution temperature for a chain population with similar *LES*,

$$T_d(r) = A - \frac{B}{LES} \quad (2)$$

where $A = T_d^o - T_S$, $B = T_d^o \times \alpha$, and T_d^o is the equilibrium dissolution temperature of a chain with infinite length (this parameter depends on solvent and polymer type), T_S is a supercooling temperature (to account for supercooling during Crystaf analysis), and α is a constant that is inversely proportional to the enthalpy of fusion. The model parameters (n, k, A, and B) for ethylene/α-olefin copolymers with several comonomer contents at various cooling rates were reported in our previous publication.[16]

Because crystallization takes place from a dilute solution, an increase in crystallinity is related to a decrease in the weight fraction of polymer remaining in solution, $C(T_C)$. We proposed a very simple equation to describe this relationship (the integral Crystaf profile) by taking the information from the weight distribution function of *LES*, $W(LES)$ into account,

$$C_{model}(T_C) = \sum_{r=1}^{\infty} (W(LES) \cdot (1 - X(LES, T_C))) \quad (3)$$

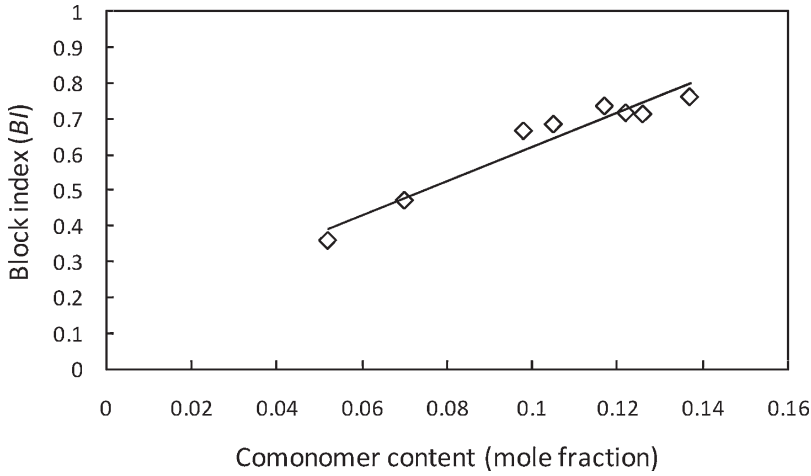

Figure 3.
Block index results for OBCs.[6]

The differential Crystaf profile can be obtained by differentiation of Equation (3) with respect to the crystallization temperature, that is, by calculating $dC_{model}(T_C)/dT_C$.

Adaptation of the Crystaf Model for OBCs

In the case of OBCs, we have assumed that the longest ethylene sequence (*LES*) in each chain remained the key factor determining chain crystallizability. This hypothesis is tentative and needs further experimental confirmation, but it provides one of the crucial pieces of information needed for the adaptation of our Crystaf model. Crystallization kinetics of each OBC chain can be calculated following the same procedure adopted for random ethylene/α-olefin copolymers. However, the additional factor that needs to be considered when simulating Crystaf profiles of OBCs is the systematic shift to higher crystallization temperatures that is observed when ATREF profiles of OBCs are compared to those of ethylene/α-olefin random

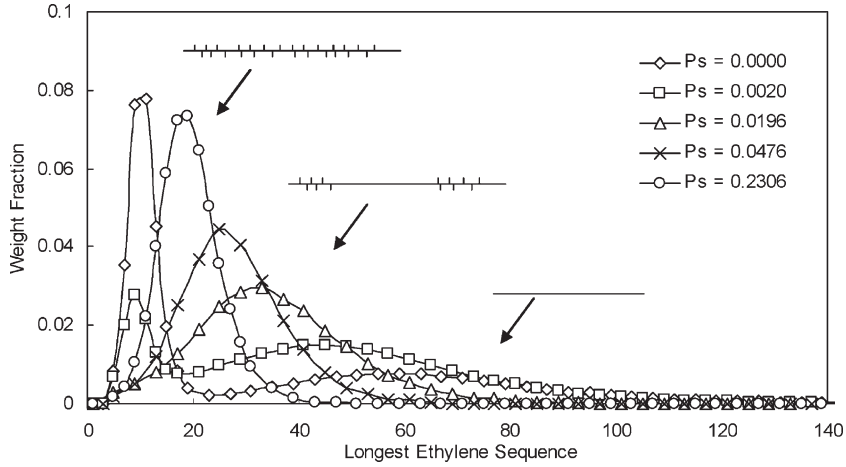

Figure 4.
Effect of chain shuttling probability on the longest ethylene sequence distribution ($P_{c,1} = 0.01$, $P_{c,2} = 0.1$, $P_{p,1} = P_{p,2} = 0.999067$, $M_n = 30$ kg/mole. Subscripts indicate catalyst type.).

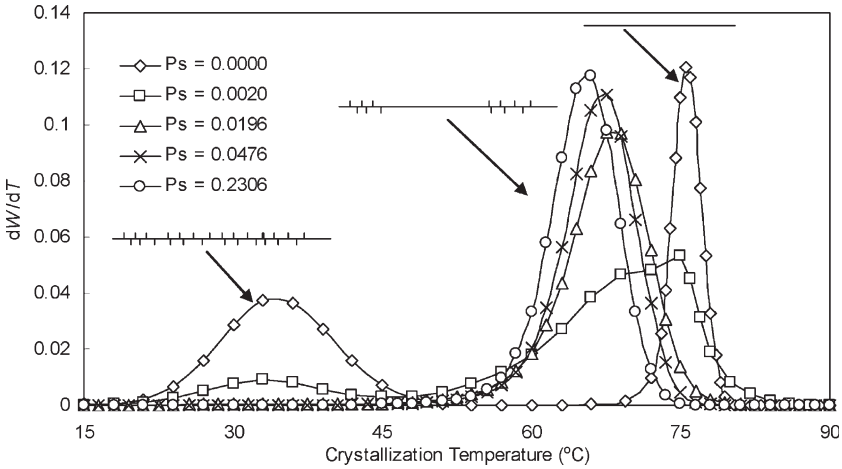

Figure 5.
Effect of chain shuttling probability on Crystaf profiles ($P_{c,1} = 0.01$, $P_{c,2} = 0.1$, $P_{p,1} = P_{p,2} = 0.999067$, $M_n = 30$ kg/mole. Subscripts indicate catalyst type.).

copolymers with the same α-olefin molar fraction. To quantify this temperature shift, we used the definition of *block index* introduced by Li Pi Shan and Hazlitt.[6]

The block index (*BI*) quantifies how the ATREF peak elution temperature of OBCs deviates from that of random ethylene/α-olefin copolymers with the same α-olefin molar fraction,

$$BI = \frac{1/T_x - 1/T_{x0}}{1/T_A - 1/T_{AB}} \quad (4)$$

where T_x is the ATREF elution temperature (T_e) of an OBC fraction of narrow chemical composition, T_{x0} is the T_e of the equivalent narrow-composition random copolymer, T_A is the T_e of chains composed of a single hard block, and T_{AB} is the T_e of a random copolymer with the same average composition of the whole OBC. When carefully examined, the degree to which the intra-chain comonomer distribution is blocked can be interpreted from this parameter; the larger the *BI*, the more ''blocky'' the polymer will be.

For the present simulations, we arbitrarily assumed that the temperature shift due to the ''blockiness'' of OBCs in Crystaf was approximately equal to that for ATREF. Therefore, the *BI* value can be used to shift the crystallization temperature from the expected crystallization temperature of the equivalent random ethylene/α-olefin copolymers (T_{x0}) to that of the OBC (T_x). This hypothesis is most likely inaccurate, but was required for simulation purposes, as *BI* results for Crystaf analysis of OBCs have not been reported in the open literature. As these results become available in the future, the simulation results reported herein can be easily updated.

For each simulated OBC chain, the average comonomer content was used to estimate block index (*BI*) using a linear relationship based on results previously reported by Li Pi Shan and Hazlitt[6] and illustrated in Figure 3,

$$BI = 4.783 \cdot CC + 0.143 \quad (5)$$

where *CC* is the mole fraction of α-olefin of the OBC chains generated via Monte Carlo simulation.

The degree of crystallinity of random ethylene/α-olefin copolymer chains with the same average comonomer content and *LES* as each simulated OBC chain obtained from Monte Carlo simulation can be calculated using Equation (1). This information, together with the *BI* estimated

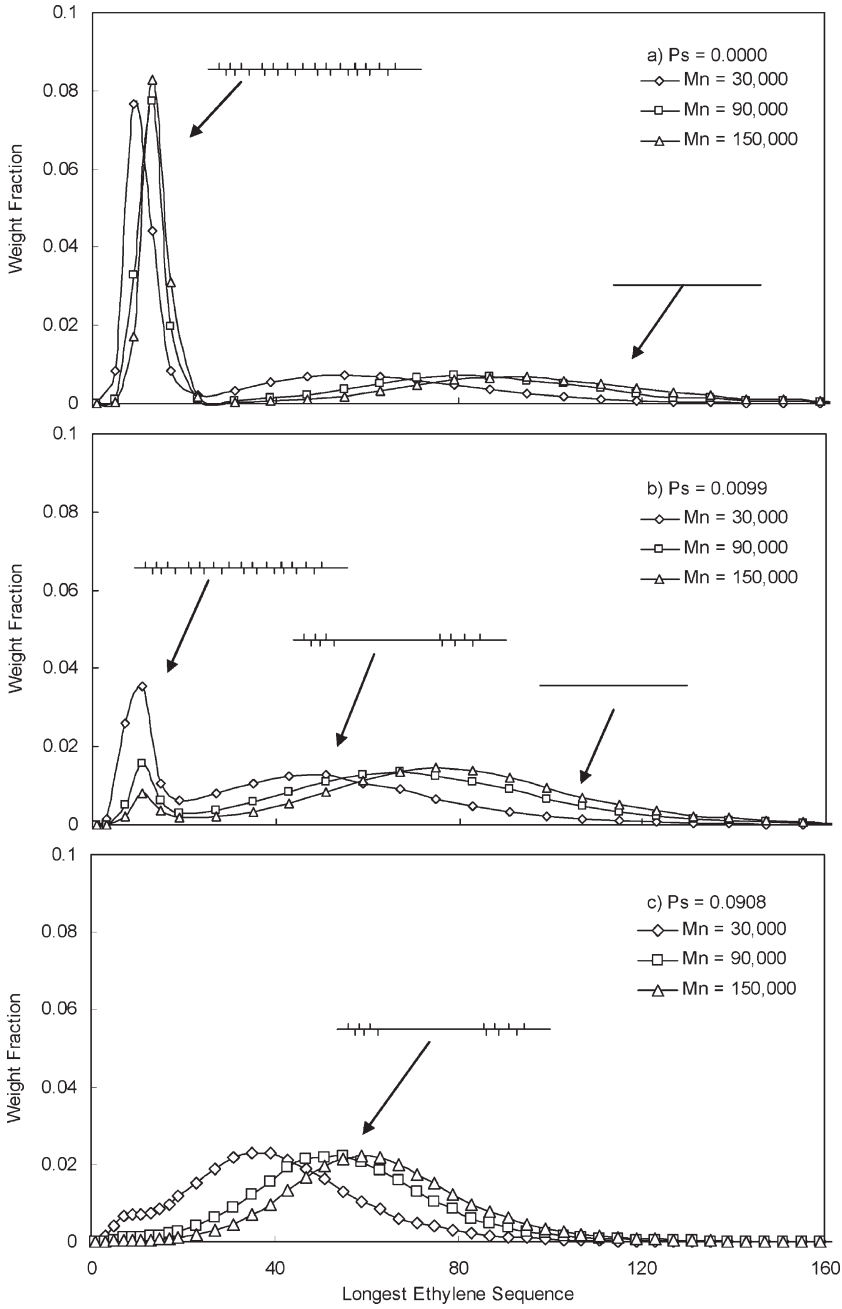

Figure 6.
Effect of molecular weight on the longest ethylene sequence distribution for several chain shuttling probabilities ($P_{c,1} = 0.01$, $P_{c,2} = 0.1$).

for each chain generated with our Monte Carlo algorithm, was used to shift the crystallization temperatures of the OBC chains and predict their Crystaf profiles.

Results and Discussion

Figure 4 illustrates the effect of the chain shuttling probability (P_s) on the *LES*

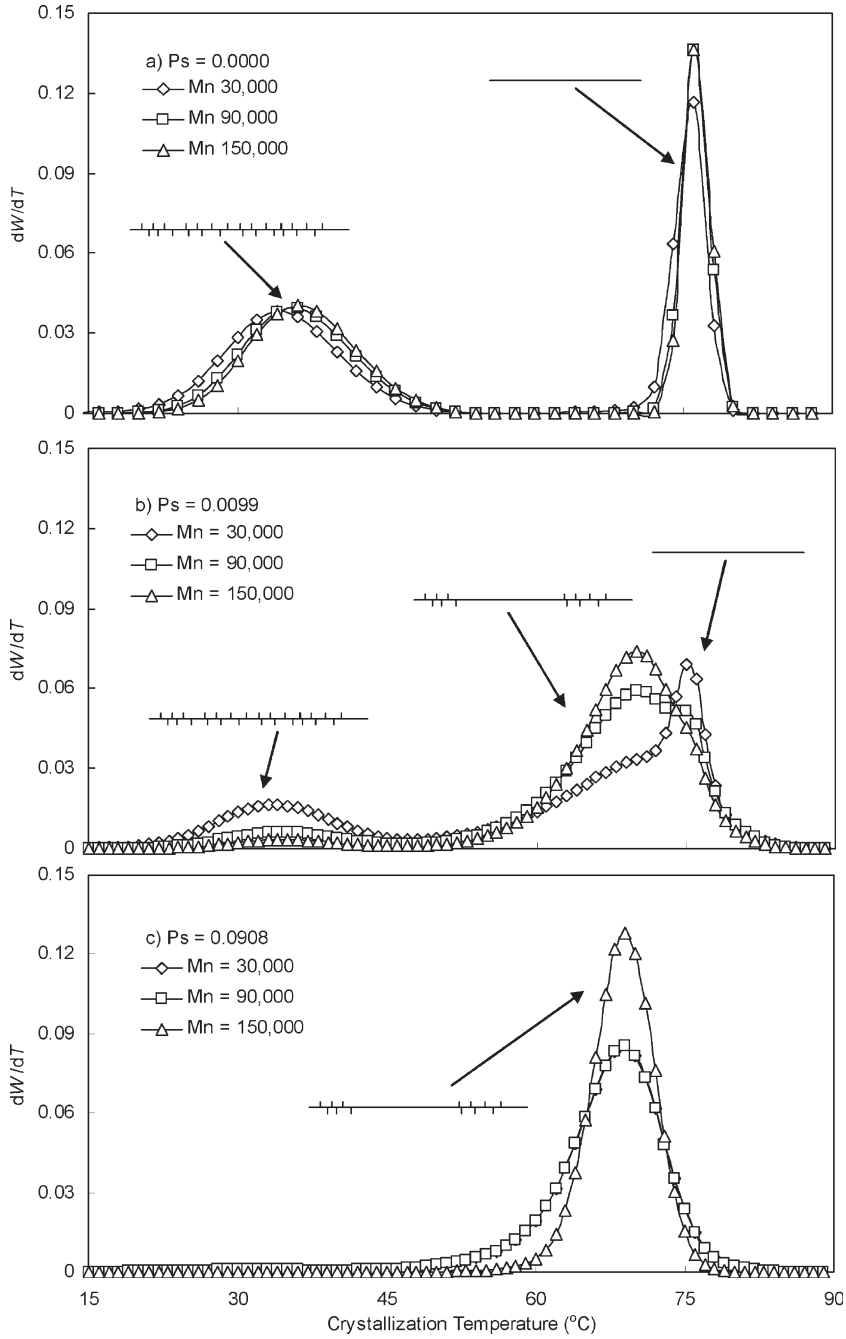

Figure 7.
Effect of molecular weight on Crystaf profiles for several chain shuttling probabilities ($P_{c,1} = 0.01$ and $P_{c,2} = 0.1$).

distribution of OBCs. Starting with $P_s = 0$ (no chain shuttling), we notice that each catalyst makes its own independent polymer population with very distinct *LES* distributions: Catalyst 1 makes ethylene-rich copolymer and, therefore, its *LES* distribution is shifted to the right (longer *LES*), while polymer made with Catalyst 2,

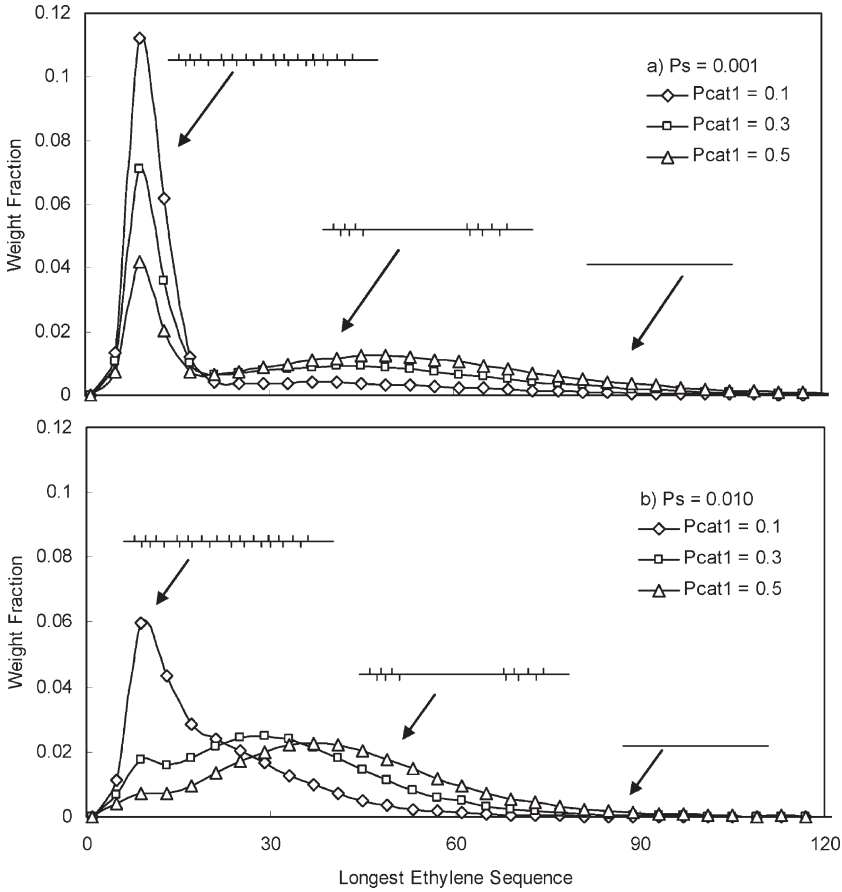

Figure 8.
Effect of mole fraction of Catalyst 1 on the longest ethylene sequence distribution for several chain shuttling probabilities ($P_{c,1} = 0.01$ and $P_{c,2} = 0.1$).

the ethylene-poor catalyst, has much shorter *LES*. With the introduction of CSA in the reactor, and consequent increase of chain shuttling frequency, these two independent polymer populations start to merge, generating a unimodal *LES* distribution with increasing P_s. It is also interesting to notice that, as P_s increases, the *LES* distribution narrows and shifts to the left, approaching the *LES* distribution of the ethylene-poor catalyst. This should be expected, as increasing the chain shuttling frequency will necessarily lead to the formation of progressively shorter polymer blocks.

The equivalent effect of chain shuttling frequency on the predicted Crystaf profiles is shown in Figure 5. Increasing chain shuttling frequency from zero to 0.2306 will make the original bimodal Crystaf profile (corresponding to a blend of polyolefins with different α-olefin fractions) to shift to narrow and unimodal Crystaf profiles.

Figure 6 and 7 illustrate the effect of changing the molecular weight on the *LES* distribution and on the predicted Crystaf curves, respectively. As already observed with random ethylene/α-olefin copolymers,[7–9] decreasing the molecular weight average will shift the *LES* distribution towards lower averages. The same phenomenon is observed for OBCs, albeit this tends to be a minor effect for high molecular weight polymers.

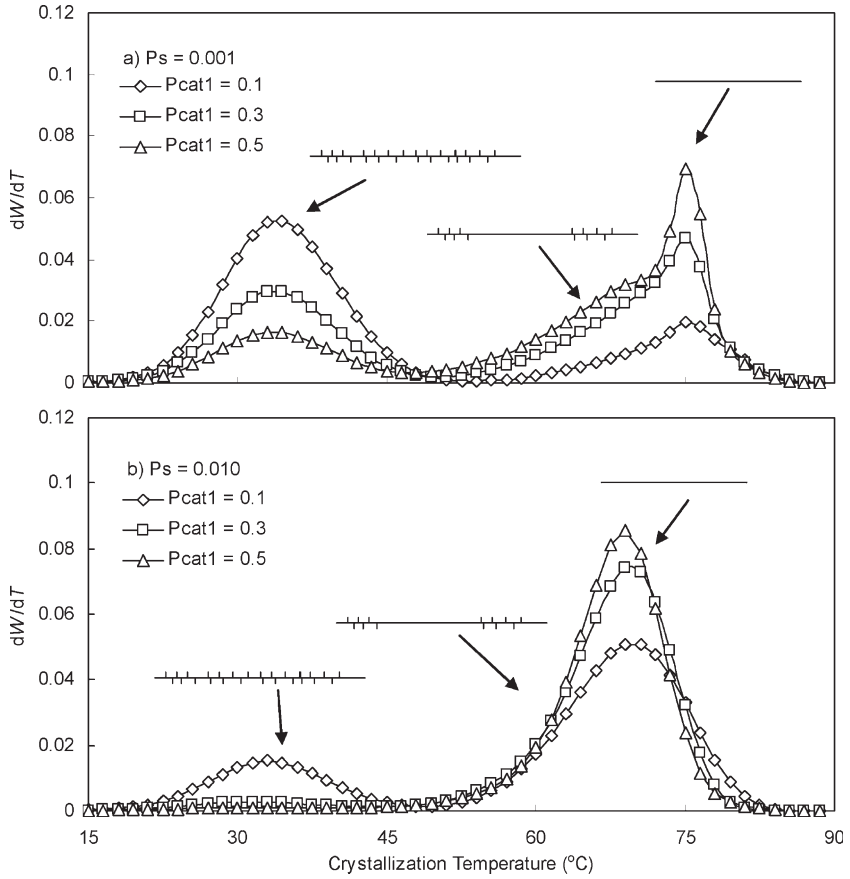

Figure 9.
Effect of mole fraction of Catalyst 1 on Crystaf profiles for several chain shuttling probabilities ($P_{c,1} = 0.01$ and $P_{c,2} = 0.1$).

Finally, Figure 8 and 9 investigate the effect of the mole fraction of Catalyst 1 in the reactor on the *LES* distribution and predicted Crystaf profiles, respectively. Not surprising, as the fraction of Catalyst 1 increases for a given probability of chain shuttling, the *LES* distribution moves towards higher averages, since Catalyst 1 was assumed to have a lower probability of comonomer incorporation than catalyst 2 ($P_{c,1} = 0.01$ and $P_{c,2} = 0.1$). It is illustrative to notice how changing the ratio of the two catalysts in the reactor can lead to the formation of products with completely different microstructures and, consequently, distinct mechanical and rheological properties. It is easy to see that this approach is a very effective way for controlling polymer properties and developing OBC formulations for new applications.

Conclusion

Crystaf profiles of OBCs produced with chain shuttling catalyst technology were simulated by combining the OBC chain microstructures generated with a Monte Carlo simulation model with a Crystaf model modified using the OBC block index. The effect of polymerization parameters (chain shuttling probability, propagation probability, and catalyst ratio) on the distribution of the longest ethylene sequence per chain and Crystaf profiles

were examined. Even though several hypothesis made in this model are yet to be tested (assuming that the block index expression derived for ATREF applies to Crystaf and that the crystallization of OBCs is mainly regulated by the longest ethylene sequence in the chains), this modeling approach offers a first glance into some properties of these fascinating materials and is useful to interpret Crystaf and ATREF results as well as to relate them to OBC chain microstructure. The model can also be applied in the future to examine the effect of polymerization parameters on OBC microstructure to fine tune process conditions to make OBCs with desired chain microstructures and properties.

Acknowledgements: Siripon Anantawaraskul thanks financial supports from the Thailand Research Fund (TRF) and Center of Excellence for Petroleum, Petrochemicals and Advanced Materials (PPAM).

[1] D. J. Arriola, E. M. Carnahan, P. D. Hustad, R. L. Kuhlman, T. T. Wenzel, *Science* **2006**, *312*, 714.
[2] T. T. Wenzel, D. J. Arriola, E. M. Carnahan, P. D. Hustad, R. L. Kuhlman, *Top Organomet Chem* **2009**, *26*, 65.
[3] D. U. Khariwala, A. Taha, S. P. Chum, A. Hiltner, E. Baer, *Polymer* **2008**, *49*, 1365.
[4] H. P. Wang, D. U. Khariwala, W. Cheung, S. P. Chum, A. Hiltner, E. Baer, *Macromolecules* **2007**, *40*, 2852.
[5] P. Gupta, S. Costeux, T. Oswald, Y. W. Cheung, L. Weaver, S. Karande, S. Chum, *ANTEC Annual Technical Conference* **2007**, *2*, 973.
[6] C. Li Pi Shan, L. G. Hazlitt, *Macromol. Symp.* **2007**, *257*, 80.
[7] S. Anantawaraskul, J. B. P. Soares, P. Jirachaithorn, J. Limtrakul, *J. Polym. Sci. Polym. Phys.* **2006**, *44*, 2749.
[8] S. Anantawaraskul, P. Jirachaithorn, J. B. P. Soares, J. Limtrakul, *J. Polym. Sci. Polym. Phys.* **2007**, *45*, 1010.
[9] S. Anantawaraskul, J. B. P. Soares, P. Jirachaithorn, *Macromol. Symp.* **2007**, *257*, 94.
[10] J. B. P. Soares, B. Monrabal, J. Nieto, J. Blanco, *Macromol. Chem. Phys.* **1998**, *199*, 1917.
[11] A. A. da Silvo Filho, J. B. P. Soares, G. B. de Galland, *Macromol. Chem. Phys.* **2000**, *201*, 1226.
[12] D. M. Sarzotti, J. B. P. Soares, A. Penlidis, *J Polym Sci Part B: Polym Phys* **2002**, *40*, 2595.
[13] D. Beigzadeh, J. B. P. Soares, T. A. Duever, *J Appl Polym Sci* **2001**, *80*, 2200.
[14] S. Costeux, S. Anantawaraskul, P. M. Wood-Adams, J. B. P. Soares, *Macromol Theory Simul* **2002**, *11*, 326.
[15] S. Anantawaraskul, J. B. P. Soares, P. M. Wood-Adams, B. Monrabal, *Polymer* **2003**, *44*, 2393.
[16] S. Anantawaraskul, P. Somnukguandee, J. B. P. Soares, J. Limtrakul, *J. Polym. Sci. Polym. Phys.* **2009**, *47*, 866.

